technische universität dortmund

Microstructured Resonators for Electron Spin Resonance

Magnetic resonance uses microwaves to excite transitions between different spin states and detects the oscillating magnetic field generated by the evolution of coherent superposition states of the spins. Excitation therefore requires the conversion of a microwave signal into an oscillating magnetic field and detection the reverse process. The efficiency of both processes can be enhanced by a suitable resonant structure, the microwave resonator. The goal of this project is the design and implementation of highly efficient resonators for small samples. For this purpose, we use planar circuits with dimensions significantly smaller than the wavelength of the microwave. We design them such that the circuit impedance is 50 Ω at the design frequency. Most of these resonators are delivered to other projects in the DFG priority program 1601, and we optimize the design for the requirements of these individual projects.

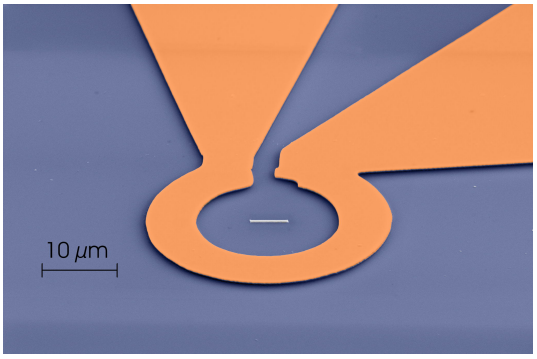

EPR resonators and sensitivity

Most implementations of electron paramagnetic resonance (EPR) use resonant structures for efficiently converting microwave signals to oscillating magnetic fields that excite transitions between electronic spin states. The same structures are also used to convert precessing magnetization into microwave signals that can be detected by the microwave bridge of the spectrometer. Both processes are most efficient if the oscillation frequency of the spins (the Larmor frequency) coincides with a resonator mode. In a standard EPR spectrometer, this structure is a cavity with conducting walls.

The condition that the Larmor frequency should coincide with a resonance frequency of the cavity imposes a relation between the dimensions of the cavity and the Larmor frequency Ω_L of the spins: $\Omega_L \approx 2\pi\kappa c/d$, where c is the velocity of light, d is a resonator dimension and κ is a numerical constant of order unity, which depends on the type of resonator chosen and the mode at which it operates. For the usual operation frequency of 9.5 GHz, a rectangular TE_{102} cavity thus has dimensions of $45 \times 22 \times 10$ mm^3, much larger than typical sample sizes. An immediate consequence of this is that the strength of the microwave magnetic field inside the resonator is relatively weak. The connection between the volume of the resonator and the amplitude B_1 of the microwave magnetic field can be seen by calculating the amplitude of the B_1 field from the energy W stored in the cavity, $W = P_{\mu w}\tau = P_{\mu w}Q/\nu_{\mu w}$, where τ is the storage time, $P_{\mu w}$ the microwave power entering the cavity, $Q = \nu_{\mu w}\tau$ is the quality factor of the resonator, and $\nu_{\mu w} = \Omega_L$ the microwave frequency. This energy is stored in the electromagnetic field, $W = \int_V d^3r\,(w_{el} + w_{mag})$, where w_{el} and w_{mag} are the electric and magnetic components of the energy density. Here, the integral runs over the volume V of the cavity. The magnetic part of the field energy density is $w_{mag} = W/(2V) = \mu_0 B_1^2$, where we have omitted the spatial variation of the magnetic field for simplicity. The field amplitude thus becomes

$$B_1 = \sqrt{\frac{W}{2V\mu_0}} = \sqrt{\frac{P_{\mu w}Q}{2V\mu_0\nu_{\mu w}}} \propto V^{-1/2}.$$

The efficiency of the conversion of microwave power to microwave magnetic field amplitude therefore decreases with increasing resonator dimensions. As we discuss below, the sensitivity follows the same relation. The efficiency of the resonator can thus be improved by reducing its size. This relation is often quantified in terms of the filling factor $\eta = V_s/V_r$, the ratio of the sample volume over the volume of the resonator. More precisely, the filling factor should be written as $\eta = \int_{sample} B_1^2 dV / \int_{-\infty}^{\infty} B_1^2 dV$ [1].

Resonator designs

While standing-wave cavities are very versatile and therefore widely used for routine applications, there are a number of possible designs that achieve higher sensitivity for small samples. Inside a material with dielectric constant ϵ, the

wavelength λ of an electromagnetic wave is reduced from its free-space value λ_0 to $\lambda = \lambda_0/\sqrt{\epsilon}$. This allows one to reduce the cavity size by inserting suitable materials with large dielectric constants [2]. This increases the filling factor significantly and thus also the sensitivity [2, 3, 4, 5]. For this purpose, low-loss ferroelectric materials are ideal, which can have dielectric constants up to 300 [5]. The resulting reduction of the resonator volume is roughly proportional to the inverse square root of the average dielectric constant, $V \propto \bar{\epsilon}^{-1/2}$.

Striplines or patch resonators [6, 7, 8] reduce the overall dimensions significantly more in the direction perpendicular to the plane of the conductor. Along the stripline or in two dimensions in the case of the patch resonator [7], the size of these resonators remains proportional to the wavelength. As in the case of the cavity resonator, their size can thus be reduced with a suitable material that combines low loss with high dielectric constant. This type of planar resonator can also be bent into a circle, as in the case of the folded half-wave resonator [9] or the slotted tube resonator [10].

For all these structures, at least one dimension is proportional to the wavelength of the microwave. This limitation was always avoided in the case of nuclear magnetic resonance (NMR), where typical wavelengths were several meters at the frequencies used in early experiments. In this case, the resonant circuits consist of lumped elements (inductive coils and capacitors), whose size can be much smaller than the wavelength. This approach also allows one to separate the electric and the magnetic components of the microwave field, with the magnetic component concentrated in the coil, while the electric component is maximized in the capacitive elements. In the context of magnetic resonance, it is mostly the concentration of the magnetic field component in the inductive element, which is used. Reducing the size of this results in efficient power-to-field conversion, i.e. a strong microwave magnetic field for a given incident power. Simultaneously, it increases the detection efficiency. This approach was transferred to the field of EPR, primarily in the form of the loop-gap resonator [11, 12, 13, 14, 15, 16].

A related approach was proposed by Ohno and Murakami [17] and by Mahdjour et al. [18], who used solenoidal microcoils to concentrate the magnetic part of the microwave field to a volume of $\approx 3 \times 0.2 \times 0.2$ mm^3. These microcoils were non-resonant, to allow excitation with different frequencies, which limited their sensitivity. Nevertheless the reported sensitivities were better than that of a conventional resonator. At the same time the use of a nonresonant coil offered fast recovery for pulsed experiments. Similar systems are used also in scanning probe microscopy, e.g. for imaging the magnetic permeability of metals with near-field microwaves [19].

Three-dimensional structures like loop-gap resonators and solenoidal coils are usually manufactured by mechanical tools. Their size is therefore limited by the precision of the available tools, typically to several hundred μm. Further size reductions are possible by moving to lithographic production techniques. This approach was introduced into EPR first in the low-frequency range at L-Band (1.4 GHz) [20], where standing-wave resonators would have volumes of liters.

Sensitivity

Sensitivity has many facets that lead to different, partly conflicting goals. In some cases, the main consideration is to obtain good signals from very dilute samples (concentration sensitivity). In other cases, one may need to detect the smallest possible number of spins. Here, we concentrate on mass-limited samples, i.e. small numbers of spins. For simplicity, we discuss the sensitivity of planar microresonators consisting of lumped circuit elements, but most of the conclusions are directly applicable to other types of resonators, such as loop-gap or cavity resonators. In the planar microresonators that we use in the present project, the sample is placed inside a small conducting loop to which we refer as the coil. The simplest approach to calculating the signal originating from the spins inside the coil starts from the voltage induced in the loop by the time-dependent flux through this coil. The signal s induced by the precessing magnetization is given by Faraday's law as $s = d\Phi/dt$, where Φ is the magnetic flux due to the spins. Since the field of a magnetic dipole decreases $\propto r^3$, with r the distance from the point dipole, while the surface of integration only grows $\propto r^2$, the signal from a point dipole in the center of the coil decreases $\propto r^{-1}$ as the coil size increases. Again, this simple model indicates that small resonators should have higher sensitivity. This scaling was also found experimentally [21].

Another approach to estimating the sensitivity uses the principle of reciprocity [22, 23], which states that the voltage ϵ induced by the precessing magnetization $\vec{M}$ in the EPR coil can be calculated by integrating the product of the magnetic field $\vec{B}_{1u}(\vec{r})$ produced by a unitary current times the transverse magnetization $\vec{M}(t,\vec{r})$ at the same place $\vec{r}$. Since the magnetic field drops $\propto d$ with the distance d from the current generating it, small resonators have higher conversion ratios, in agreement with the discussion in section . The value for the precessing magnetization $\vec{M}$ can be estimated for pulsed experiments by the static equilibrium magnetization M_0. For cw experiments, $\vec{M}(t,\vec{r})$ is given by the stationary amplitude of the transverse magnetization.

The detection limit of a resonator is obtained by comparing the signal with the thermal noise $N_{RMS} = \sqrt{4k_BTR\Delta\nu}$, where R is the input impedance of the detection apparatus - in our case the microwave preamplifier, and $\Delta\nu$ is the

detection bandwidth. In relevant applications, the detection system has an input impedance of 50 Ω. Acquisition of the signal from the sample is thus optimized if, the resonator impedance is also 50 Ω. In an optimized system, the thermal noise limit at room temperature is then $N_{RMS}(T = 300\,\mathrm{K}) \approx 0.9\,\mathrm{nV}\sqrt{\Delta\nu}$.

Design considerations

Over the last 10 years, we designed and tested microresonators for a large number of different applications.

We found that the most efficient approach for many cases was a circuit that combines lumped elements with sections of microstrip lines integrated on a suitable substrate in such a way that it could be manufactured by standard lithographic techniques. Two examples of such resonators are shown schematically in Fig. 1. The circuit elements used in these resonators can be adjusted to different sample sizes and different resonance frequencies. Reducing the size of the coil where the strongest magnetic field is generated increases the magnetic field strength in this area. As discussed below, this implies that also the spin number sensitivity for a sample in this region increases. Besides excellent power conversion and high sensitivity, these planar microresonators have a number of additional advantages. As open structures, they offer easy mechanical and optical access to the sample space and are therefore well compatible with other techniques, such as scanning probes or optical detection schemes. The spatial separation of the magnetic and electrical fields provides good compatibility with conducting samples.

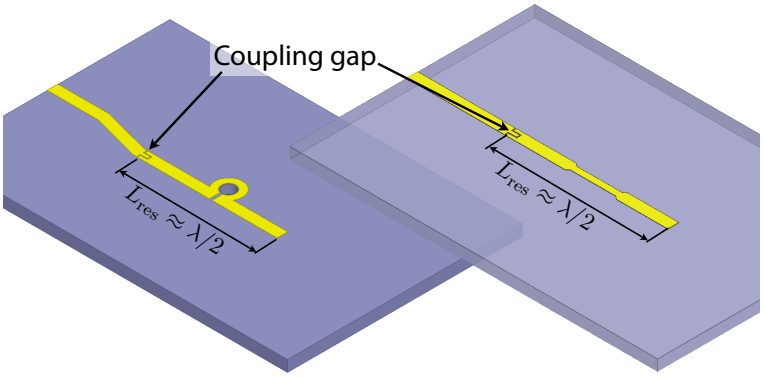

Figure 1: Schematic representation of the layout of two types of planar microresonators.

Sensitivity tests

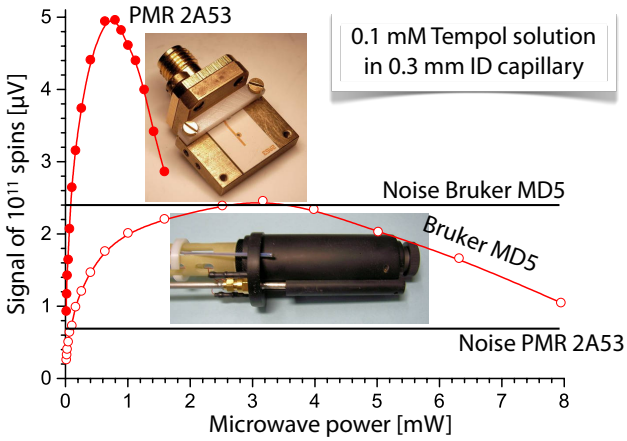

Figure 2: Sensitivity comparison between a 500 µm PMR and the Bruker MD5 resonator. The sample was an 0.3 mm inner diameter capillary filled with a solution of TEMPOL.

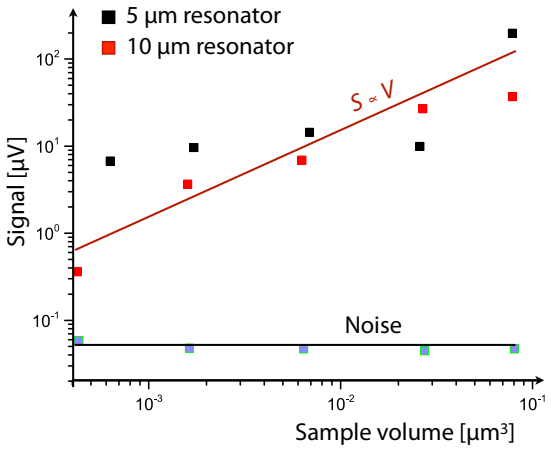

Figure 3: Signal from ferromagnetic nanostructures measured with a 5 µm and a 10 µm resonator. The straight line indicates the expected proportionality between signal and sample volume.

For a quantitative comparison with standard resonators, we compared the sensitivity of a 500 µm PMR resonator with that of a widely used resonator from Bruker, the model MD5. Figure 2 compares the measured sensitivity for a TEMPOL

sample. The solution was placed in a capillary with an 0.3 mm inner diameter. The sensitivity is maximized for the PMR for a microwave power that is approximately one order of magnitude smaller than for the Bruker resonator, and its peak value is about twice that of the Bruker resonator.

The spin number sensitivity of a microresonator increases with decreasing diameter. This was again verified by comparing the signal from resonators with different size for the same nanostructure (results not shown here). A very interesting series of measurements explored the sensitivity limits for small samples: we compared the signal from a series of cobalt-nanodots, grown by lithographic techniques in the Helmholtz-center Dresden-Rossendorf. As shown in Figure 3, the signal is roughly proportional to the sample size. The smallest sample measured in this series of experiments was a nanodot with a radius of 21 nm and a height of 100 nm, corresponding to a sample volume of $V = \pi \cdot 21^2 \cdot 100\,\mathrm{nm}^3 = 1.4 \cdot 10^{-22}\,\mathrm{m}^3$. Using the density of cobalt, ρ_{Co} = 8900 kg/m^3, this corresponds to $n = \rho_{Co} V / m_{Co} \approx 10^7$ spins.

We also tested microstrip resonators as detectors for samples with quasi-1D shapes. We could show that they work. Compared to resonators with loop structures and comparable dimensions, the spin-number sensitivity was about an order of magnitude lower. This is in agreement with expectations, since the microwave magnetic field of these structures extends over a significantly larger volume.

Tuner for microresonators

The PMR's produced in this project are optimized to work at a specific resonance frequency and the parameters are chosen such, that at this resonance frequency, most of the microwave power from the transmission line enters the resonator, while the reflection is minimized. In some cases, small deviations between the targeted and the actual device lead to shifts of the resonator frequency from the target frequency or they result in reflections at the target frequency that exceed the level of -30 dB considered to be ideal for ESR resonators. Some of these deviations can be compensated by placing dielectric materials at specific points of the resonators. This approach is, however, limited and cannot be done while the resonator is operated in the spectrometer.

As an alternative that allows tuning under operation, we developed a movable shield that is placed over the resonator and can be adjusted by a micrometer screw to optimize the coupling between the feedline and the resonator. Figure 4 shows a sketch of the design.

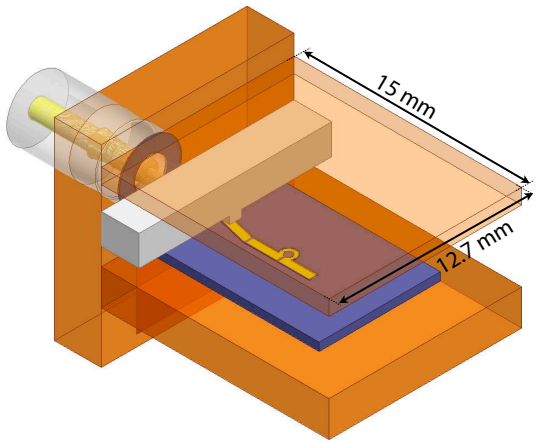

Figure 4: Design of tuner for microresonators. The position of the tuning plate, which is transparent in the figure, is adjustable by a micrometer screw.

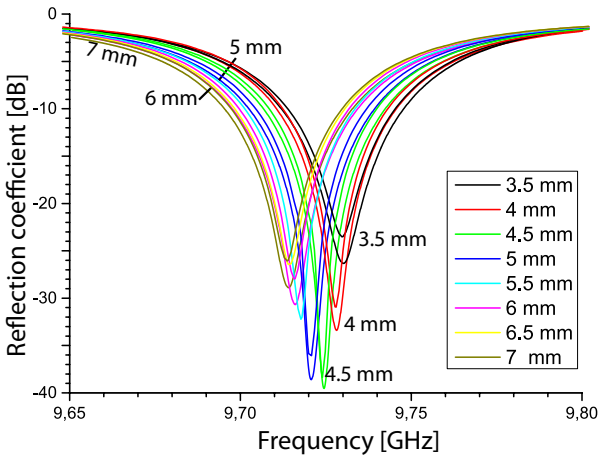

Figure 5: Experimental reflection curves of a resonator for different settings of the tuner.

Figure 5 shows a series of experimental tuning-curves measured for different distances between the shield and the resonator. Clearly, the adjustment allows one to optimize the coupling, resulting in an optimal reflection of the order of -39 dB.

As an additional benefit, the tuner also reduces radiation losses and therefore increases the sensitivity. As a fraction of the total dissipated power, the radiative losses can be written as [24]

$$\frac{P_r}{P_t} = \frac{64 Z_0 \pi h^2}{3\epsilon' Z \lambda_0^2}.$$

Here, $Z_0 \approx 377\,\Omega$ represents the impedance of free space, $Z = 50\,\Omega$ the characteristic impedance of the resonator, λ_0 the free-space wavelength and h this thickness of the substrate. For the resonators on sapphire substrates, radiative losses are of the order of 50 % of the total loss. This contribution is mostly eliminated by the tuner, and the Q-factor rises from 75 to about 102 with the tuner.

Sapphire substrates

A significant contribution to the overall losses of the PMRs is the dielectric loss in the substrate, which depends mostly on the loss tangent of the substrate material. We therefore evaluated the losses from existing designs and looked for low-loss substrates. We found that sapphire is a very interesting material, since it almost completely eliminates dielectric losses, as shown in table 1. The values Q_d listed in the table can be estimated as

$$Q_d = \frac{\epsilon_{eff}(\epsilon_r - 1)}{\epsilon_r(\epsilon_{eff} - 1)} \frac{1}{\tan\delta}.$$

Material	Q_d
TMM	530
Silicon	810
Sapphire	15000

Table 1: Dielectric loss for different substrate materials.

Here, $\epsilon_r \approx 10$ is the dielectric permittivity of the microstrip substrate and $\epsilon_{eff} \approx 6.5$ is the weighted dielectric permittivity of the microstrip line, taking into account the materials, including the air, over which the field extends.

The optimized designs for the sapphire substrates are very similar to those used on TMM substrates, but the parameters had to be adjusted for the new material. Initial tests of these resonators showed that their quality factor is indeed significantly higher than for resonators manufactured on TMM. This improvement results not only from the lower loss substrate material, but also from the higher surface quality, which also reduces conductive losses from surface roughness. Measurement in partner laboratories, e.g. MPI Mühlheim, confirmed a significant gain in sensitivity.

Resonant metamaterials for high-frequency applications

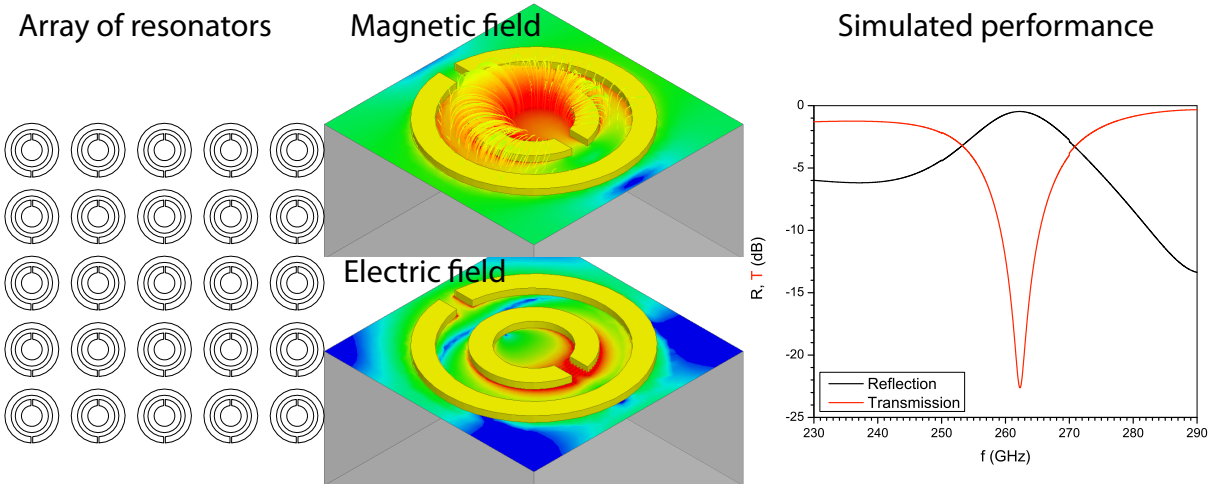

Figure 6: Left: Array of split-ring resonators designed to enhance the incoming microwave field in the region of the plane. Center: simulated field distribution for a single resonator. Right: simulated reflection and transmission curves as a function of frequency.

Microresonators can be designed for all frequencies used in EPR. However, for high frequencies (typically above 35 GHz), the losses in the transmission lines become too high for useful operation. Resonant structures could nevertheless prove useful even in the case of free-space in-coupling, e.g. by enhancing the microwave field in the sample region. In collaboration with the group of Alexander Schnegg (Helmholtz-Zentrum Berlin), we therefore designed structures that achieve this for frequencies of 260 GHz and 445 GHz. Initial experiments showed indeed a resonant enhancement in the expected frequency range.

Ferromagnetic nanostructures

The design of future spintronic devices requires a quantitative understanding of the microscopic linear and nonlinear spin relaxation processes governing the magnetization reversal in nanometer-scale ferromagnetic systems. Ferromagnetic resonance is the method of choice for a quantitative analysis of relaxation rates, magnetic anisotropy and susceptibility in a single experiment. In conventional resonators, such measurements could only be performed on ensembles of nanostructures [25], but the planar microresonators manufactured in this project allow us to perform measurements on single nano-structured devices.

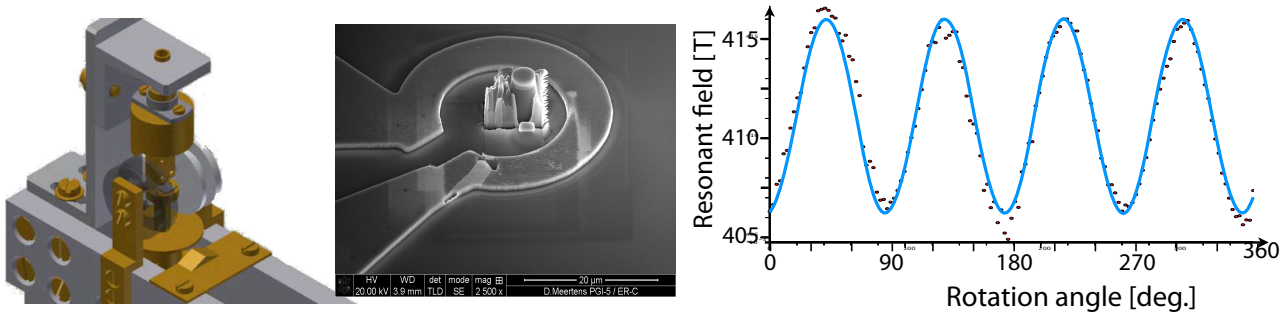

Figure 7: Left: Schematic representation of the setup for rotating microresonators with samples. Center: SEM image of a mesocrystal inside the resonator. Right: Measured variation of the EPR frequency with the rotation angle for the sample shown in the center, using the setup shown at left.

Nano-structured samples show pronounced anisotropies, making orientation-dependent measurements very attractive. Since these samples are too small to rotate inside the resonators, we designed a setup that allows us to rotate sample and resonator together inside the magnet. Figure 7 shows a schematic representation of the setup, an SEM image of a mesocrystal, consisting of ferromagnetic nano-particles, and the measured variation of the EPR resonance field with the rotation angle. The observed periodicity of 90^{deg} is consistent with the cubic structure of the mesocrystal. The amplitude of the anisotropic component is small (10 mT at a mean value of 410 mT) but highly significant. A full analysis of the result will require additional measurements, including different frequencies.

A cryoreceiver for EPR

One of the possible ways for increasing the sensitivity of magnetic resonance detection is to reduce the temperature of the sample; a closely related option is the reduction of the receiver temperature, to reduce the Nyquist noise, which depends mostly on the temperature of the first stage in the receiver chain.

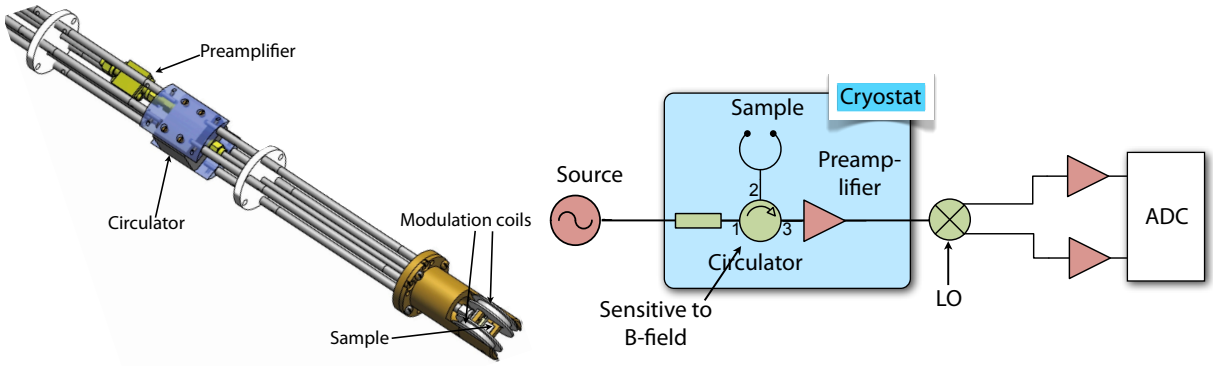

Figure 8: Left: Schematic representation of the mechanical part of the cryoreceiver. Right: Electronic scheme of cryoreceiver.

We therefore designed and implemented such a receiver. One major difficulty was that the noise temperature is also limited by the temperature of the circulator. Since this part is sensitive to magnetic fields, it cannot be placed as close to the sample as it should be for optimal sensitivity and is therefore usually placed outside of the cryostat, at room

temperature. To reduce its temperature and to reduce the distance from the sample, we used a shielded circulator that can sustain magnetic fields up to 50 mT and placed it in the cryostat, at about 20 cm from the sample, where the magnetic field does not exceed 50 mT. The preamplifier was mounted close to the cryostat, such that the two devices could be cooled to ≈ 20 Kelvin. Figure 8 shows a schematic drawing of the setup on the left-hand side. The right-hand side shows the electronic design, with the cooled part of the setup marked by the blue box.

Figure 9 shows the noise measured from this setup as a function of temperature. The blue curve corresponds to the expected noise floor from thermal noise, $P_{th} = k_B T \Delta f$, where Δf is the receiver bandwidth. The red curve includes, in addition to the theoretical thermal noise, also the contribution from the input noise of the preamplifier, which was measured independently. This curve, which is not a fit to the data, is in excellent agreement with the experimental data (red and black squares). These data clearly show that the concept works and that the increase of the S/N agrees with the theoretical expectation.

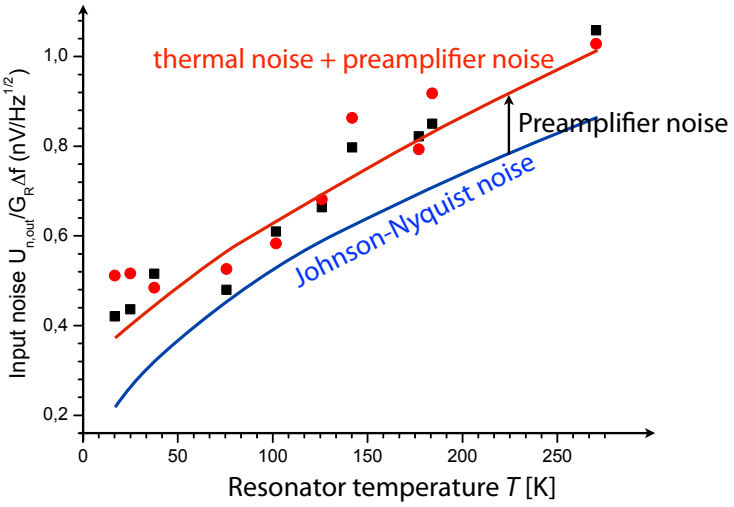

Figure 9: Experimental noise from the cryoreceiver measured against temperature of the resonator.

References

[1] C. P. Poole, *Electron spin resonance* (John Wiley, 1982).

[2] M. Jaworski, A. Sienkiewicz, and C. P. Scholes, J. Magn. Reson. **124**, 87 (1997).

[3] R. W. Dykstra and G. D. Markham, J. Magn. Reson. **69**, 350 (1986).

[4] I. Golovina, I. Geifman, and A. Belous, J. Magn. Reson. **195**, 52 (2008).

[5] Y. E. Nesmelov, J. T. Surek, and D. D. Thomas, J. Magn. Reson. **153**, 7 (2001).

[6] B. Johansson, S. Haraldson, L. Pettersson, and O. Beckman, Rev. Sci. Instrum. **45**, 1445 (1974).

[7] W. J. Wallace and R. H. Silsbee, Rev. Sci. Instrum. **62**, 1754 (1991).

[8] J. L. Davis and W. B. Mims, Rev. Sci. Instrum. **49**, 1095 (1978).

[9] C. P. Lin, M. K. Bowman, and J. R. Norris, J. Magn. Reson. **65**, 369 (1985).

[10] M. Mehring and F. Freysoldt, J. Phys. E: Sci. Instrum. **13**, 894 (1980).

[11] J. S. Hyde, W. Froncisz, and T. Oles, J. Magn. Reson. **82**, 223 (1989).

[12] J. W. Sidabras, R. R. Mett, W. Froncisz, T. G. Camenisch, J. R. Anderson, and J. S. Hyde, Rev. Sci. Instrum. **78**, 034701 (2007).

[13] S. Pfenninger, J. Forrer, A. Schweiger, and T. Weiland, Rev. Sci. Instrum. **59**, 752 (1988).

[14] B. Simovic, P. Studerus, S. Gustavsson, R. Leturcq, K. Ensslin, R. Schuhmann, J. Forrer, and A. Schweiger, Rev. Sci. Instrum. **77**, 064702 (2006).

[15] R. D. Britt and M. P. Klein, J. Magn. Reson. **74**, 535 (1987).

[16] W. Froncisz and J. S. Hyde, J. Magn. Reson. **47**, 515 (1982).

[17] K. Ohno and T. Murakami, J. Magn. Reson. **79**, 343 (1988).

[18] H. Mahdjour, W. Clark, and K. Baberschke, Rev. Sci. Instrum. **57**, 1100 (1986).

[19] S.-C. Lee, C. P. Vlahacos, B. J. Feenstra, A. Schwartz, D. E. Steinhauer, F. C. Wellstood, and S. M. Anlage, Applied Physics Letters **77**, 4404 (2000).

[20] G. Boero, M. Bouterfas, C. Massin, F. Vincent, P.-A. Besse, R. S. Popovic, and A. Schweiger, Rev. Sci. Instr. **74**, 4794 (2003).

[21] R. Narkowicz, D. Suter, and I. Niemeyer, Rev. Sci. Instrum. **79**, 084702 (2008).

[22] D. I. Hoult and R. E. Richards, J. Magn. Reson. **24**, 71 (1976).

[23] D. Hoult, Progr. NMR Spectr. **12**, 41 (1978).

[24] B. Easter and R. Roberts, Electronics Letters **6**, 573 (1970), ISSN 0013-5194.

[25] P. H. Bryant, J. F. Smyth, S. Schultz, and D. R. Fredkin, Phys. Rev. B **47**, 11255 (1993).